Determination of Kinetic Constants for the Interaction between a Monoclonal Antibody and Peptides Using Surface Plasmon Resonance†

Danièle Altschuh,* Marie-Christine Dubs, Etienne Weiss,‡ Gabrielle Zeder-Lutz, and Marc H. V. Van Regenmortel
Institut de Biologie Moléculaire et Cellulaire, Laboratoire d'Immunochimie, 15 rue Descartes, 67084 Strasbourg Cedex, France
Received September 24, 1991; Revised Manuscript Received April 9, 1992

ABSTRACT: Differences in the affinity of a monoclonal antibody raised against the protein of tobacco mosaic virus for 15 related peptides (residues 134–146) carrying single-residue modifications were investigated using a novel biosensor technology (Pharmacia BIAcore). Analysis of the peptide–antibody interaction in real time allowed fast and reproducible measurements of both association and dissociation rate constants. Out of 15 mutant peptides analyzed, five were not recognized by the antibody at all, and seven were recognized as well as the wild-type peptide. For three of the peptides, the rate constants were different for the mutant and wild-type peptides. The pattern of residue recognition suggests that the epitope is formed by three residues (140, 143, and 144) in a helical conformation that mimics the structure in the protein. Even a minor modification of these residues totally abolishes recognition by the antibody. Modifications of adjacent residues result in small but significant differences in association and/or dissociation rate constants. One of the recognized residues is totally buried in the three-dimensional structure of TMV protein, suggesting that a structural rearrangement next to the helix occurs during protein–antibody interaction.

The molecular basis of the specificity of antigen–antibody interactions is still poorly understood. This is due partly to the difficulty of analyzing in detail the nature of the molecular contacts. Crystallographic analysis provides detailed structural information about the size of interacting surfaces and the nature of potential contacts. However, not all residues found at a distance suitable for interaction participate equally in the binding energy. The effective role of each residue can only be ascertained by analyzing the effect of its modification on the interaction.

The BIAcore system (Pharmacia Biosensor AB, Uppsala, Sweden) allows a quantitative analysis of molecular interactions in real time. Therefore, association and dissociation rate constants can be readily calculated. The system uses surface plasmon resonance (SPR) (Kretschmann & Raether, 1968), a quantum mechanical phenomenon, which detects changes in optical properties at the surface of a thin gold film on a glass support (sensor surface) (Löfås & Johnsson, 1990). The sensor surface carries a dextran matrix on which one of the two reactants is covalently attached. The other is introduced in a flow passing over the surface. Resonance occurs at a specific angle of incident light. The resonance angle depends on the refractive index in the vicinity of the metal surface and is monitored continuously, thus allowing the association or dissociation of molecules from the sensor surface to be followed in real time. No labeling of the ligands is required.

This paper describes a functional analysis of the interaction between a monoclonal antibody raised against tobacco mosaic virus (TMV) protein and a peptide corresponding to residues 134–146 of this protein. Differences in binding affinity resulting from single substitutions in the peptide were measured using the biosensor technology.

Experimental Procedures

Equipment and Reagents. Large amounts of monoclonal antibody 57P raised against TMV protein (Al Moudallal et al., 1985) were obtained in cell culture. The antibody was purified on a protein A Sepharose column (Pharmacia). Its concentration was determined by optical density at 280 nm using an absorption coefficient of 1.4.

The wild-type peptide corresponding to residues 134–146 of TMV protein, and 15 related peptides carrying single residue substitutions were synthesized by the solid-phase method of Merrifield (Barany & Merrifield, 1980). Peptide purity was controlled by HPLC and by determination of amino acid composition as described previously (Briand et al., 1989). All peptides were at least 80% pure. Table I lists the 16 peptide sequences. The peptides will be referred to by the nature and position of the change (e.g., Y139F referring to the peptide with Tyr 139 replaced by Phe).

The instrument (BIAcore system) and reagents for interaction analysis were obtained from Biosensor AB, Uppsala, Sweden. The reagents include sensor chips CM5, surfactant P20, *N*-hydroxysuccinimide (NHS), *N*-ethyl-*N'*-[(3-dimethylamino)propyl]carbodiimide hydrochloride (EDC) and ethanolamine-HCl.

ELISA Inhibition Assays. Inhibition tests were performed as described previously (Altschuh & Van Regenmortel, 1982). Coating of the wells was done with 500 ng/mL TMV protein. Mab 57P was used as ascitic fluid diluted 1/100000. Peptide inhibitor concentrations ranged between 0 and 10 μg/mL.

Immobilization of Peptides on the Sensor Surface. Standard procedures described previously (Löfås & Johnsson, 1990; Fägerstam et al., 1990) were used for immobilization. The ligand is concentrated on the carboxylated dextran matrix by an ion exchange effect at pH below the isoelectric point of the ligand and covalently coupled via primary amino groups. In our case, only a low peptide concentration could be reached in the dextran matrix, probably due to the hydrophobic nature of the peptide, and a relatively high concentration of peptide had to be used in order to immobilize the desired amount. All peptides behaved similarly except peptide F144V for which the efficiency of immobilization was increased about 10-fold. The immobilization run was performed at a flow of 5 μL/min in HBS, pH 7.4 [10 mM Hepes, 0.15 M NaCl, 3.4 mM ethylenediaminetetraacetic acid disodium salt (EDTA), 0.05%

† This work was supported by grants to M.H.V.V.R. from the Institut National de la Santé et de la Recherche Médicale (INSERM), the Conseil Régional d'Alsace, and the Fondation Médicale.
* Author to whom correspondence should be addressed.
‡ Present address: Ecole Supérieure de Biotechnologie de Strasbourg, 11 rue Humann, 67085 Strasbourg Cedex, France.

0006-2960/92/0431-6298$03.00/0

Table I: Sequence of Wild-Type and Mutant Peptides

	position												
	134	135	136	137	138	139	140	141	142	143	144	145	146
WT	Arg	Gly	Thr	Gly	Ser	Tyr	Asn	Arg	Ser	Ser	Phe	Glu	Ser
S138A					Ala								
S138N					Asn								
Y139F						Phe							
N140K							Lys						
N140S							Ser						
S142A									Ala				
S142N									Asn				
S142T									Thr				
S143A										Ala			
S143T										Thr			
F144V											Val		
E145D												Asp	
E145A												Ala	
S146A													Ala
S146D													Asp

surfactant 20]. The carboxylated matrix was first activated with 30–35 μL of an EDC/NHS mixture. Peptide (20–40 μL) at a concentration of 1–3 mg/mL in formate buffer, pH 3.0 or 3.5, was injected. Unreacted groups were blocked by the injection of 30 μL of ethanolamine-HCl, pH 8.5, followed by 15 μL of 50 mM NaOH to remove noncovalently bound peptide.

Theory of Kinetic Measurements. The symbols used are those of Hardie and Van Regenmortel (1975): A, total antigen concentration; s, antigen valence; As, total antigen sites; B, total antibody concentration; n, antibody valence; Bn, total antibody sites; y, bound antibody concentration; ny, bound sites; d, free antibody concentration; nd, free antibody sites.

In the analysis presented here, the peptide antigen was immobilized on the dextran matrix of the sensor surface. A known concentration of antibody was injected in a constant flow.

The reaction rate between peptide and antibody results from the difference between molecules that associate and molecules that dissociate in every unit of time. Association is a function of association rate constant (k_a) and free ligand concentration. Dissociation is a function of dissociation rate constant (k_d) and concentration of the complex. Using the above symbols, the reaction rate as a function of free and bound molecules can be described by

$$\mathrm{d}ny/\mathrm{d}t = k_a(As - ny)(Bn - ny) - k_d ny \quad (1)$$

where As − ny = free antigen sites, Bn − ny = free antibody sites, and ny = bound sites.

In the BIAcore system, antibody reaches the surface in a constant flow. Hence the concentration of free antibody sites, usually expressed as total minus bound sites (Bn − ny), is a constant corresponding to the concentration of antibody sites in the flow (nd). If we replace (Bn − ny) by (nd) and expand eq 1, we obtain a first-order equation of the reaction rate as a function of complex formed:

$$\mathrm{d}ny/\mathrm{d}t = k_a(As)(nd) - ny(k_a nd + k_d) \quad (2)$$

A plot of $\mathrm{d}ny/\mathrm{d}t$ versus ny yields a straight line from which k_a can be obtained from its intercept on the vertical axis. k_d can be obtained from its slope.

A linear relationship also exists between the slope of this plot and antibody concentration.

$$\text{slope} = k_a nd + k_d \quad (3)$$

When the reaction is studied at several antibody concentrations, the slope value of each $\mathrm{d}ny/\mathrm{d}t$ versus ny plot can be used to construct a new plot of slope value versus antibody concentration (eq 3); k_a and k_d can be deduced from the slope and intercept of this new plot. In this case, the concentration of antigen sites (As) on the surface is not needed.

Experimental Values for Kinetic Measurements. Equations 2 and 3 can be expressed in terms of measurements made during BIAcore kinetic runs as follows (Karlsson et al., 1991, 1992). (1) The molar concentration of injected antibody (d) must be known. (2) In the case of peptides and monoclonal antibodies, the antigen valence $s = 1$. (3) When antibody is injected in small successive amounts, as is the case in a flow, its binding to a multivalent viral antigen tends to be bivalent (Van Regenmortel & Hardie, 1976). In the conditions used for our kinetic runs, it was found that the high concentration of peptide in the dextran was also conducive to bivalent binding (Karlsson et al., 1992). Thus the antibody valence $n = 2$. (4) Total number of antigenic sites available on the dextran matrix (As) is determined by the maximum amount of antibody that can be bound to the surface and is expressed in resonance units (RU). This amount will be called y_{max}. Thus $As = ny_{max}$. (5) The reaction rate ($\mathrm{d}y/\mathrm{d}t$) and bound antibody (y) are both given by the BIAcore software at chosen intervals of time. They will be called $\mathrm{d}R_A/\mathrm{d}t$ (RU s^{-1}) and R_A (RU) respectively. The refractive index change (R) at a given time is the sum of refractive index from bulk solution (R_{RI}), immobilized ligand (R_L), and antibody bound to the immobilized ligand (R_A) (Karlsson et al., 1991). In a kinetic run, R_A is obtained simply by substracting from the total response (R), the value ($R_{RI} + R_L$), which is a constant. R_L corresponds to the baseline value before antibody injection (report point 1 in Figure 2a). R_{RI} corresponds to the difference between report points 5 and 4 in Figure 2a. The translated eq 2 reads

$$\mathrm{d}R_A/\mathrm{d}t = k_a 2y_{max}d - R_A(k_a 2d + k_d) \quad (4)$$

Thus

$$k_a = \text{intercept}/2y_{max}d \quad (5)$$

$$k_d = \text{slope} - \text{intercept}/y_{max} \quad (6)$$

When studying the interaction at different antibody concentrations eq 3 becomes

$$\text{slope} = k_a 2d + k_d \quad (7)$$

Kinetic Runs. Monoclonal antibody 57P at concentrations ranging from 10 to 100 nM in HBS was allowed to interact with sensor surfaces on which the different peptides had been immobilized. The runs were performed at 25 °C, at a flow rate of 3 μL/min during 7 min (21-μL injection), taking report points (for $\mathrm{d}R_A/\mathrm{d}t$ and R_A values) every 10 s. After the run, the surface was regenerated by injecting a 50 mM HCl solution during 2 min (6-μL injection). The instrument software

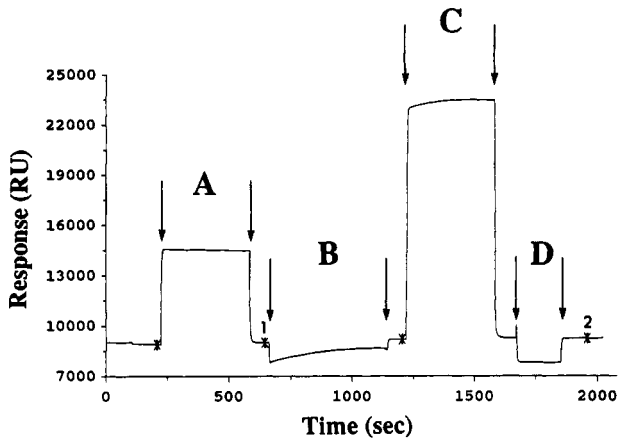

FIGURE 1: Sensorgram showing the immobilization of peptide Y139F on the sensor surface (experiment 2 of Table II). The flow rate is 5 μL/min. (A) Activation of the carboxylated dextran matrix by the injection of 30 μL of EDC/NHS mixture. The beginning and end of injection are indicated by arrows. The large variations in RU observed at the beginning and end of injection correspond to the difference in refractive index between the injected material and the buffer. Report points are always taken during buffer flow in between two injections. (B) Injection of 40 μL of a 1 mg/mL solution of peptide in formic acid pH 3.5. (C) Inactivation of unreacted groups by 35 μL of ethanolamine. (D) Washing off noncovalently bound peptide with 30 μL of 50 mM NaOH. The 249 RU difference in resonance units between report points 1 and 2 corresponds to immobilized peptide.

produces a table of dR_A/dt and R_A values that can be directly used in a plotting program (Microsoft Excel).

BIAcore Inhibition Assays. The wild-type peptide was immobilized on the sensor surface as described above. Fourteen microliters of 100 nM Mab solution in HBS was injected at a 7 μL/min flow rate. The surface was regenerated by injecting 5 μL of 50 mM HCl. The antibody response in the absence of peptide inhibitor is 800 RU and corresponds to about 90% of surface saturation. For inhibition assays, Mab 57P was mixed before injection with various peptides at concentrations ranging from 50 nM to 10 μM.

RESULTS

Peptide Immobilization. Optimal conditions for kinetic runs (Karlsson et al., 1991) require the presence of a low concentration of antigen on the matrix, so that there are no mass transport limitations and so that the reaction reaches equilibrium within reasonable time limits (less than 15 min). Accurate values of reaction rates are obtained if the rate is larger than 0.25 RU s^{-1}. To meet these conditions, the amount of peptide immobilized was adjusted so that the antibody response at surface saturation would be between 300 and 1500 RU. The expected ratio of antibody to peptide response at saturation can be calculated because RUs are proportional to refractive index increment and thus to the mass of protein. In the case of bivalent antibody binding, this ratio should be 75000 RU of antibody (MW 150000) for 1200 RU of peptide (MW 1200) or 750/12. At least 50–500 RU of peptide had to be immobilized on the sensor surface in order to obtain adequate antibody binding, suggesting that not all peptide molecules were available for antibody binding or alternatively that a fraction of the peptide was inactive. Because the number of antigen sites is measured indirectly by the maximum amount of antibody bound at saturation, inactive antigen sites are not taken into account in calculations. Figure 1 shows a typical immobilization plot for peptide Y139F.

Conditions Used for Kinetic Measurements. Figures 2 and 3 show the various steps that were performed for each peptide analyzed, taking as an example the interaction between Mab

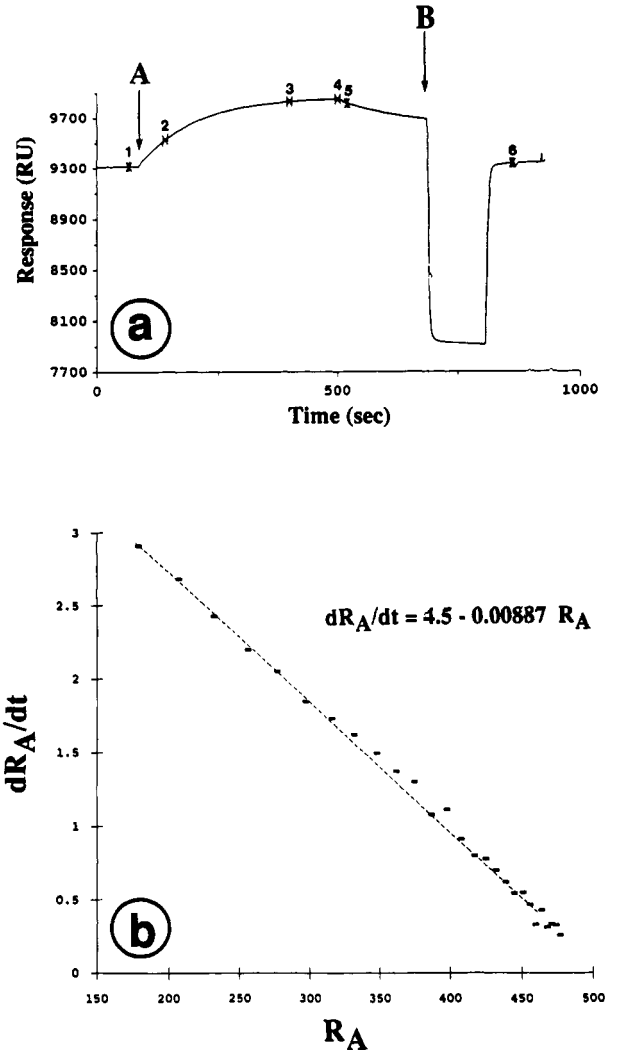

FIGURE 2: Example of a typical kinetic run analysis (experiment 2 of Table II) using eq 4. A total of 249 RU of peptide Y139F is immobilized on the sensor surface. (a) Kinetic run at a 37.5 nM concentration of Mab 57P. (A) 21 μL of antibody followed by (B) 6 μL of 50 mM HCl is injected at a flow rate of 3 μL/min. Report points for dR_A/dt and R_A values are taken every 10 s between 60 s (report point 2) and 420 s (report point 4) after antibody injection. For clarity of the sensorgram, locations of all report points are not shown. Reaction rates are below 0.25 RU s^{-1} following 320 s of Mab injection (after report point 3) and are not used in panel b. The difference in resonance units between report points 4 and 5 (33 RU) corresponds to the difference in refractive index between buffer and antibody solution, and this value is used to correct the antibody response R_A. (b) dR_A/dt versus R_A plot. Values taken every 10 s between time 60 and 320 s are included.

57P and peptide Y139F immobilized as shown in Figure 1. Figure 2a is a typical kinetic run at an antibody concentration of 37.5 nM. The corresponding reaction rate (dR_A/dt) versus bound antibody (R_A) is given in Figure 2b. A plot of steady-state value (antibody bound at equilibrium) as a function of antibody concentration (Figure 3a) shows that the maximum amount of antibody that can be bound to the surface (y_{max}) is 740 RU. From these data obtained at a 37.5 nM concentration of Mab, the following values of $k_a = 8.1 \times 10^4$ s^{-1} M^{-1} and $k_d = 2.8 \times 10^{-3}$ s^{-1} were obtained from eqs 5 and 6. Kinetic runs were performed at concentrations ranging from 10 to 100 nM. The average k_a and k_d values at several concentrations were $k_a = 7.7 \times 10^4$ s^{-1} M^{-1} and $k_d = 2.6 \times 10^{-3}$ s^{-1}. When using the slope versus antibody concentration plot (eq 7, Figure 3b), the slope and intercept gave $k_a = 7.9 \times 10^4$ s^{-1} M^{-1} and $k_d = 2.6 \times 10^{-3}$ s^{-1}. In this case, y_{max} (Figure 3a)

Table II: Example of k_a and k_d Values Obtained in Four Independent Experiments for the Interaction between Peptide Y139F and Monoclonal Antibody 57P

			mean values obtained using eq 4 (6–7 Mab dilutions)			values obtained using eq 7		
data	RU peptide immobilized	y_{max}	k_a ($\times 10^4$) (M^{-1} s^{-1})	k_d ($\times 10^{-3}$) (s^{-1})	K_a ($\times 10^7$) (M^{-1})	k_a ($\times 10^4$) (M^{-1} s^{-1})	k_d ($\times 10^{-3}$) (s^{-1})	K_a ($\times 10^7$) (M^{-1})
1	179	630	9.0 ± 0.9	2.4 ± 0.5	3.7	8.9	2.5	3.6
2	249	740	7.7 ± 0.6	2.8 ± 0.5	2.8	7.9	2.6	3.0
3	151	657	6.7 ± 0.4	2.4 ± 0.3	2.7	7.2	2.0	3.6
4	193	546	7.4 ± 0.5	2.5 ± 0.3	2.9	7.2	2.8	2.6
mean			7.7 ± 1.0	2.5 ± 0.2		7.8 ± 0.8	2.5 ± 0.3	

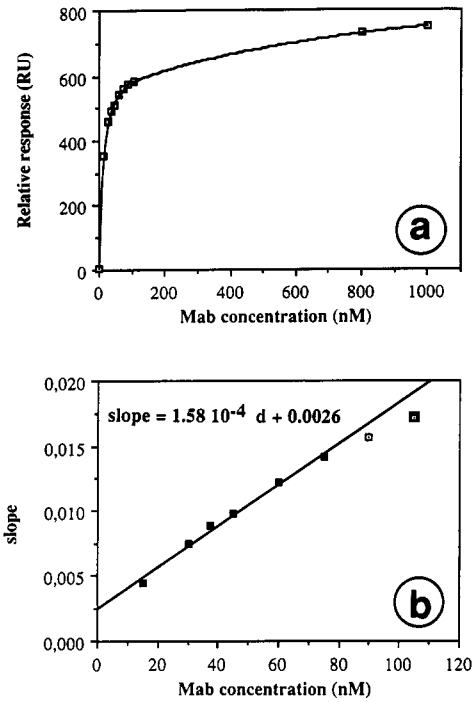

FIGURE 3: Example of plots obtained in a typical calculation using eq 7 (experiment 2 of Table II). (a) Bound antibody at equilibrium (RU) versus antibody concentration (nM), showing the y_{max} value of 740 RU. Bound antibody at equilibrium is given by report point 5 (Figure 2a) in 10 kinetic runs at various antibody concentrations. (b) Slope value of plots shown in Figure 2b versus antibody concentration.

is not needed. Figure 3b shows that antibody concentrations leading to an equilibrium value close to saturation of the surface (Figure 3a) cannot be used, because the plot clearly deviates from linearity at antibody concentrations above 80 nM. Concentrations leading to an equilibrium value below 80% of surface saturation were used for rate constant calculations.

Reproducibility of Kinetic Measurements. A large number of independent experiments were performed to test the reproducibility of kinetic measurements done with the biosensor technology. Table II summarizes the results obtained in four experiments measuring the interaction between peptide Y139F and Mab 57P. In the example shown, deviations from the mean for association rate constants calculated at different Mab concentrations within one experiment were comprised between 6% and 13.5%, while those for dissociation rate constants were between 12% and 21%. Errors calculated on the mean values obtained in several independent experiments were of the same order of magnitude. Such an extensive analysis would not be needed routinely. In our experience, the first method (eq 4) gives reliable results when antibody concentrations are used that correspond to the steep part of the equilibrium RU value versus antibody concentration curve (Figure 3a). Thus two

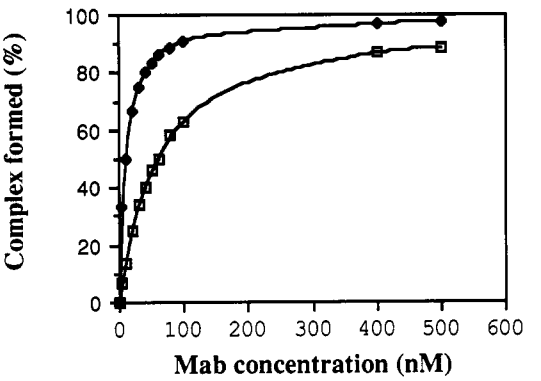

FIGURE 4: Theoretical plots of complex formed at equilibrium as a function of Mab concentration. The plots were obtained from modeling the interaction between Mab 57P and peptide Y139F (◆) or S142N (□). Complex formed is expressed as the percentage of maximum antigen binding sites available on the sensor surface.

runs at high antibody concentration for determination of y_{max} and two or three kinetic runs at lower concentrations for k_a and k_d calculations are sufficient for each peptide. The second method (eq 7) is more economic in antibody since y_{max} is not needed and is also advisable for low-affinity interactions where y_{max} may be difficult to determine. However, at least six kinetic runs at appropriate antibody concentrations must be performed. In particular, the k_d value is very sensitive to small variations in the slope of the plot as shown in Figure 3b. In the example shown, the chosen Mab concentrations were slightly too high, since the corresponding steady-state values are close to surface saturation (Figure 3a), so that the two highest concentrations (90 and 105 nM) could not be used.

Once k_a and k_d have been approximately defined in preliminary kinetic runs, experimental conditions can be easily optimized by modeling the interaction curves using the integrated version of eq 4 and the experimental parameters (antigen and antibody concentrations and observed kinetic constants). Concentrations to be used experimentally can be derived from theoretical plots of the percentage complex formed at equilibrium as a function of Mab concentration. Figure 4 illustrates such plots for the binding of Mab 57P to peptides Y139F and S142N. The equilibrium binding constant (Figure 5c) is only about three times lower for peptide S142N (10^7 M^{-1}) than for peptide Y139F (3×10^7 M^{-1}). Figure 4 shows that Mab concentrations between 0 and 100 nM are optimal for kinetic runs with peptide S142N, but slightly too high in the case of peptide Y139F since the last four points are above 80% of surface saturation. The plots in Figure 4 also show that only 89% of the antigenic sites are saturated at a 500 nM Mab concentration in the case of peptide S142N, while 98% are saturated in the case of peptide Y139F. Relatively large amounts of antibody would thus be needed in order to determine surface saturation for antibodies with affinity below 10^7 M^{-1}. Similarly kinetic plots (complex formed as a function of time) can also be modeled in order

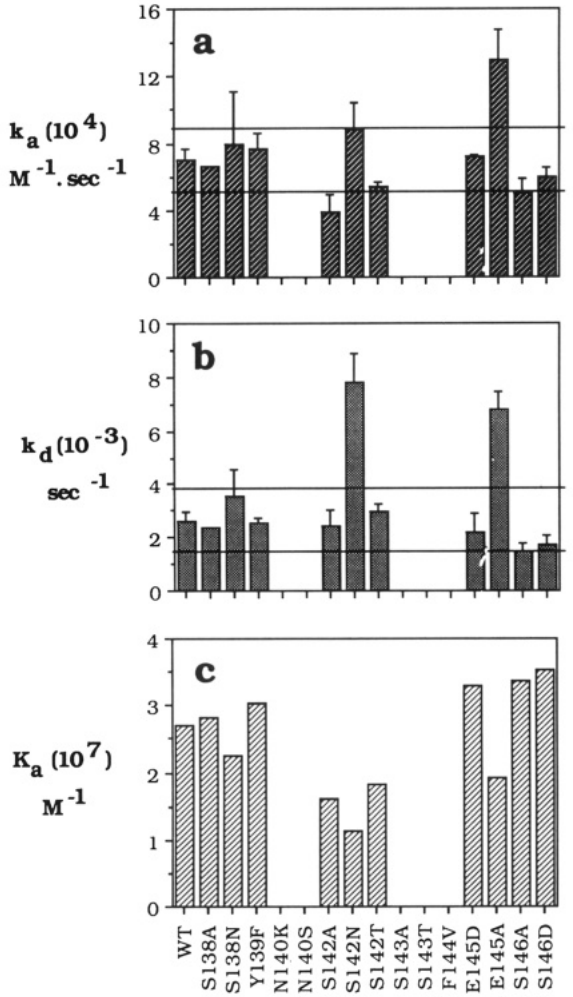

FIGURE 5: Comparison of the kinetic rate constants and equilibrium constants of Mab 57P for the 16 peptides. Error bars for k_a and k_d values correspond to the deviation from the mean in independent experiments (two to four experiments performed on different sensor surfaces).

to define the time of Mab injection required to reach equilibrium for various k_a and k_d values.

Results of Kinetic Measurements. Using the two methods described above, k_a and k_d values were calculated for the wild-type peptide and 15 mutant peptides. Except for peptide S138A, each measurement was done at least twice and up to four times on different surfaces. The immunoreactivity in solution of all peptides was verified by their capacity to inhibit the interaction between Mab 57P and the wild-type peptide either in ELISA or BIAcore assays. Results of kinetic experiments, obtained using eq 4, are summarized in Figure 5 as histograms for association rate constant (Figure 5a), dissociation rate constant (Figure 5b), and equilibrium binding constant (Figure 5c). Error bars represent deviations from the mean obtained in independent experiments. These errors are larger than average for peptide S138N because we were unable to immobilize this peptide in sufficient amounts. As a consequence, antibody values at saturation were low (less than 300 RU).

Substituted peptides were considered significantly different from wild-type peptide when the differences were greater than three times the standard deviation obtained for the wild type, shown as horizontal lines on the histograms. Thus, among peptides that bind to the antibody, three show significant differences in binding to Mab 57P, as compared to the unmodified peptide: peptide S142A has a slightly slower association rate constant, peptide S142N a faster dissociation rate constant, and peptide E145A faster association and dissociation rate constants. Inhibition ELISA tests gave the following results: at a 5 μg/mL concentration of peptide inhibitor, peptide S142N inhibited the reaction between TMV protein and Mab 57P to about 50%, peptide E145A to about 70%, and peptide S142A to 90% as does the wild type. The same ranking was obtained when inhibition tests were performed with the BIAcore (Figure 6). The 1600 nM peptide concentration corresponds to a 8-fold molar excess over antibody sites. It seems that the peptides with the highest inhibitory capacity tend to have the lowest dissociation rate constants (Figure 5b). However, the number of peptides is too small and the measured k_d values too similar to be able to draw a general rule. The kinetic parameters of peptide E145A differ most from those of the wild type, since both association and dissociation rate constants are affected. However, in solution this peptide behaves closer to the wild type than peptide S142N. This example illustrates the importance of a kinetic analysis of the interaction.

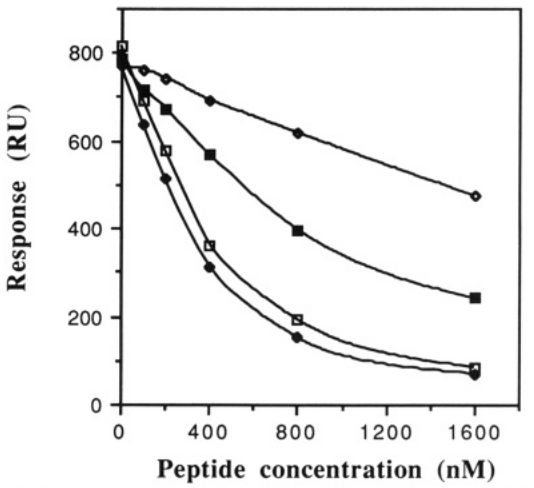

FIGURE 6: Immunoreactivity in solution of the wild-type peptide (□), peptides S142A (◆), S142N (◇), and E145A (■). The binding (expressed in resonance units) of a 100 nM solution of Mab 57P to the wild-type peptide coupled to a sensor surface is inhibited with various amounts of the peptides.

Five peptides show no interaction at all with the antibody in kinetic experiments: N140K, N140S, S143A, S143T, and F144V. Coupling to the sensor surface could lead to inactivation of the peptide, particularly for peptide N140K, which can be immobilized through the ϵ-amino group of the lysine residue, as well as through the N-terminal amino group. Inhibition assays on the BIAcore were performed to test the immunoreactivity of these peptides in solution. The wild-type peptide inhibits the interaction between antibody and immobilized peptide to 55% at a 2-fold molar excess of peptide over antibody. No inhibition was detected at a 50-fold molar excess of peptides N140K, S143T, or F144V. However, in these conditions peptides N140S and S143A inhibited the interaction to about 20%. It is possible to calculate the response expected in the conditions used for kinetic measurements. Such a calculation shows that an interaction with $K_a = 10^5$ M^{-1} would yield a response of 80 RU only at the highest Mab concentration used (500 nM), if k_a is larger than 10^3 $M^{-1} \times s^{-1}$. Interactions with smaller association rate constants will not give a significant response within the 7 min injection time.

DISCUSSION

Structural Characterization of the Epitope Recognized by Monoclonal Antibody 57P. Out of 15 modifications tested,

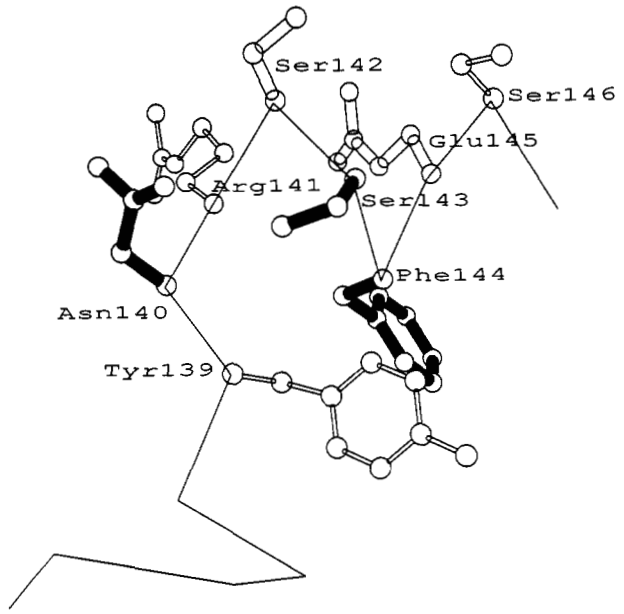

FIGURE 7: Picture of the crystallographic structure of region 134–146 in TMV protein (Bloomer et al., 1978). Side chains of essential residues are shown in thick black lines. Side chains of residues whose modification results in small variations in affinity are shown in thick white lines. Other residues are in thin white lines. Side chains of residues Arg 141, Glu 145, and Phe 144 point down, while others point up.

seven had no effect on the interaction, five totally prevented binding (N140K, N140S, S143A, S143T, and F144V), and three produced an intermediate effect (S142A, S142N, and E145A). Thus, three residue side chains were essential for antibody recognition: Asn 140, Ser 143, and Phe 144. It seems, therefore, that the equilibrium binding constant of 2.7×10^7 M^{-1} calculated for the interaction between the wild-type peptide and antibody 57P (Figure 5c) results from a very small surface of interaction. The location of the epitope in the region 140–144 is consistent with results obtained by Trifilieff et al. (1991) using pepscan plates. These authors showed that Mab 57P was able to bind hexapeptides 139–144 and 140–145, indicating that some or all residues 140–144 are involved in recognition by Mab 57P. Furthermore, substitution of Asn 140 by Arg on TMV protein (mutant CP415) was also found to prevent binding of antibody 57P (Dore et al., 1987). Other mutations in the region 140–144 of the protein are not available.

Our data suggest that the interaction between peptide 134–146 and monoclonal antibody 57P is not only sequence specific but also conformation specific. Modifications that totally prevent antibody binding occur at three positions (140, 143, and 144), two of which are not contiguous in the sequence. Position 141 has not been tested, but position 142 clearly plays only a minor role in binding, while even subtle modifications at position 143, such as removal of a hydroxyl group (S143A) or addition of a methyl group (S143T), abolish the interaction. In the crystallographic structure of TMV protein, residues 141–148 form a short α-helix (Bloomer et al., 1978; Mondragon, 1984) on which Ser 143 is spatially contiguous to Asn 140 (Figure 7). The side chain closest to Ser 143 on the next helix turn is Ser 147, which is not part of the epitope since peptide 136–148, which is two residues longer on the C-terminal end, binds the antibody similarly to peptide 134–146 (results not shown). Side chains contiguous to Asn 140 and Ser 143 on either side of the helix cylinder are those of Ser 142 on one side and Tyr 139 and Phe 144 on the other side (Figure 7). Ser 142 plays only a minor role in antibody binding. The Phe 144 to Val change prevents antibody binding. Since the three essential residues are contiguous in space in the protein structure, we suggest that the epitope is formed by residues Asn 140, Ser 143, and Phe 144 in their helical conformation. Whether a conformation of the peptide exists in solution or is induced by binding to the antibody is not known.

Functional Characterization of the Epitope. In the example analyzed here, the effect on interaction of residue modifications is rarely modulated, but results in either total absence of binding or binding equal to that observed with the wild type. A functional interaction between peptide and antibody probably results in our case from a cooperative effect of several bonds between antigen and antibody and not from the addition of independent effect. This behavior might follow from the extremely small size of the epitope. In a large surface of interaction, removal of a bond should result in a smaller difference in affinity that corresponds to the specific contribution of that particular bond.

The nature of modifications at positions 142 and 145 that produce small variations in k_a or k_d suggests indirect effects rather than direct contribution to the binding affinity. Changing Ser 142 to Ala only slightly decreases the association rate constant, indicating that a hydrogen bond between Ser 142 and the antibody is not essential. There is also no strict shape complementarity since the additional methyl group of a Thr side chain has no effect. The Ser 142 to Asn modification results in a similar association rate, but 4 times faster dissociation rate constant. This could be explained by steric strain introduced next to the contact zone by the longer Asn side chain, since Ser 142 is contiguous with the essential Ser 143.

The behavior of mutant E145A is also in favor of a structured state of the peptide in the antibody combining site. Our hypothesis in designing mutants at position 145 was that a salt bridge between Arg 141 and Glu 145 could stabilize a conformation of the peptide and that preventing the salt bridge formation could affect antibody binding. Replacing Glu 145 by Asp has no effect on the interaction. When Glu 145 is replaced by Ala, both association and dissociation rate constants are faster, while the overall association binding constant is similar to that of the unmodified peptide. Our interpretation is that peptide E145A has a larger degree of conformational freedom due to the absence of internal bonds. A higher flexibility will facilitate association, if binding involves a conformational adaptation of the antigen and/or antibody combining site, but will also facilitate dissociation. This observation is consistent with the "zipper" model for molecule interaction discussed by Burgen et al. (1975). In this model, binding occurs in successive steps involving a series of conformational rearrangements of the ligand. The overall binding constant is similar to that of the more structured ligand since the final result is the same in both cases.

Epitope Recognized on the Protein. The association rate constant for the interaction between tobacco mosaic virus protein and Mab 57P could not be calculated precisely because the interaction curve shows heterogeneous binding (results not shown), presumably because the protein is present on the sensor surface as various types of aggregates. However, dissociation from the protein is clearly much slower than dissociation from the peptide. An explanation is that the smaller conformational freedom of the epitope on the protein results in a tighter interaction.

Residue modification clearly shows that one of the residues essential for binding is Phe 144, which is totally buried in the

crystallographic structure of the protein. Thus, despite a conformational requirement for recognition, a local structural rearrangement next to the helix, in particular of Tyr 139, seems necessary for antibody binding to the protein. Evidence that Mabs are able to recognize buried residues has been presented previously (Geysen et al., 1988; Getzoff et al., 1988). In the absence of a crystallographic structure of a complex between Mab57P and TMV protein, it is difficult to know if Phe 144 is indeed directly involved in binding and what conformation of the protein is recognized.

The equilibrium binding constant between two molecules can be measured in a variety of ways, as long as the complex can be separated from free ligand once the reaction has reached equilibrium. However, few methods allow the analysis of the interaction in real time and thus the determination of kinetic rate constants. The kinetics of antigen–antibody interactions has been monitored indirectly by fluorescence techniques (Blond-Elguindi & Goldberg, 1990; Larvor et al., 1991; Foote & Milstein, 1991). The biosensor technology provides a direct means to follow the formation of complex as a function of time, thus producing highly informative interaction curves as shown in Figure 2a. Although the absolute values of the kinetic rate constants obtained when one reactant is immobilized may differ from the values measured in solution, the type of comparative studies of peptide analogues presented here is not affected by such operational differences.

Our results emphasize the importance of quantitative kinetic measurements that allow a functional and dynamic analysis of the interaction rather than a purely structural and static characterization of the epitope. As discussed elsewhere (Van Regenmortel, 1989), the notion of epitope is a functional concept and binding measurements play an essential role in the operational definition of protein epitopes.

References

Al Moudallal, Z., Briand, J. P., & Van Regenmortel, M. H. V. (1985) *EMBO J. 4*, 1231–1235.

Altschuh, D., & Van Regenmortel, M. H. V. (1982) *J. Immunol. Methods 50*, 99–108.

Barany, G., & Merrifield, R. B. (1980) in *The Peptides. Analysis, Synthesis, Biology, Vol. 2, Special Methods in Peptide Synthesis* (Gross, E., & Meienhofer, J., Eds.) pp 3–285, Academic Press, New York.

Blond-Elguindi, S., & Goldberg, M. E. (1990) *Biochemistry 29*, 2409–2417.

Bloomer, A. C., Champness, J. N., Bricogne, G., Staden, R., & Klug, A. (1978) *Nature 276*, 362–373.

Briand, J.-P., Van Dorsselaer, A., Raboy, B., & Muller, S. (1989) *Pept. Res. 2*, 381–388.

Burgen, A. S. V., Roberts, G. C. K., & Feeney, J. (1975) *Nature 253*, 753–755.

Dore, I., Altschuh, D., Al Moudallal, Z., & Van Regenmortel, M. H. V. (1987) *Mol. Immunol. 24*, 1351–1358.

Fägerstam, L. G., Frostell, Å., Karlsson, R., Kullman, M., Larson, A., Malmqvist, M., & Butt, H. (1990) *J. Mol. Recognit. 3*, 208–214.

Foote, J., & Milstein, C. (1991) *Nature 352*, 530–532.

Getzoff, E. D., Tainer, J. A., Lerner, R. A., & Geysen, H. M. (1988) *Adv. Immunol. 43*, 1–98.

Geysen, H. M., Mason, T. J., & Rodda, S. J. (1988) *J. Mol. Recognit. 1*, 32–41.

Hardie, G., & Van Regenmortel, M. H. V. (1975) *Immunochemistry 12*, 903–908.

Karlsson, R., Michaelsson, A., & Mattsson, L. (1991) *J. Immunol. Methods 145*, 229–240.

Karlsson, R., Altschuh, D., & Van Regenmortel, M. H. V. (1992) in *Structure of Antigens* (Van Regenmortel, M. H. V., Ed.) pp 127–148, Telford and CRC Press, Boca Raton, FL.

Kretschmann, E., & Raether, H. (1968) *Z. Naturforsch. A23*, 2135–2136.

Larvor, M.-P., Djavadi-Ohaniance, L., Friguet, B., Baleux, F., & Goldberg, M. E. (1991) *Mol. Immunol. 28*, 523–531.

Löfås, S., & Johnsson, B. (1990) *J. Chem. Soc., Chem. Commun. 21*, 1526–1528.

Mondragon, A. (1984) Ph.D. thesis, University of Cambridge.

Trifilieff, E., Dubs, M. C., & Van Regenmortel, M. H. V. (1991) *Mol. Immunol. 28*, 889–896.

Van Regenmortel, M. H. V. (1989) *Immunol. Today 10*, 226–272.

Van Regenmortel, M. H. V., & Hardie, G. (1976) *Immunochemistry 13*, 503–507.